INSTITUTE OF PHYSICS PUBLISHING JOURNAL OF PHYSICS B: ATOMIC, MOLECULAR AND OPTICAL PHYSICS

J. Phys. B: At. Mol. Opt. Phys. **36** (2003) 33–46 PII: S0953-4075(03)39479-9

Acceleration of the chemical reaction of trapped Ca^+ ions with H_2O molecules by laser excitation

K Okada[1], M Wada[2], L Boesten[1], T Nakamura[2], I Katayama[3] and S Ohtani[4]

[1] Department of Physics, Sophia University, 7-1 Kioicho, Chiyoda, Tokyo 102-8554, Japan
[2] Atomic Physics Laboratory, RIKEN, 2-1 Hirosawa, Wako, Saitama 351-0198, Japan
[3] Institute of Particle and Nuclear Studies (IPNS), High Energy Accelerator Research Organization (KEK), 1-1 Oho, Tsukuba, Ibaraki 305-0801, Japan
[4] Institute for Laser Science (ILS), University of Electro-Communications, 1-5-1 Chofugaoka, Chofu, Tokyo 182-8585, Japan

Received 8 July 2002, in final form 23 October 2002
Published 20 December 2002
Online at stacks.iop.org/JPhysB/36/33

Abstract

The reactivity of laser-excited Ca^{+*} ions in 3 $^2D_J (J = 3/2, 5/2)$ states with neutral H_2O molecules was experimentally investigated. The reaction-product ions were sympathetically cooled by laser-cooled $^{40}Ca^+$ ions and detected by laser-induced fluorescence mass spectroscopy. The reaction rate coefficient of $Ca^{+*}(D_J) + H_2O \rightarrow$ *products* was found to be $1.8(1) \times 10^3$ s^{-1} Pa^{-1} at an ion temperature of $T = 3.1(1) \times 10^3$ K. The ion temperature dependence of the reaction rate coefficient was also measured for buffer-gas-cooled Ca^+ ions.

1. Introduction

Over the last decade, laser cooling of trapped atomic ions has been applied to various fields of research, such as optical frequency standards based on high-resolution spectroscopy, quantum computations by manipulation of atomic coherent states and dynamics of non-neutral plasma [1–6]. In addition to these applications, sympathetic cooling is also a notable application of laser cooling. For example, it provides new ways to study ion–molecule reactions at very low energy [7–10] and precision spectroscopy of cold atomic and molecular ions [11–14]. Since ion–molecule reactions in the very low energy range play an important role in the chemical processes of interstellar space and planetary atmospheres, an investigation of the sympathetic cooling technique will also be useful for studies in the fields of astrophysics as well as chemical physics [15–18].

In frequency standard applications, however, a chemical reaction with a residual gas is a nuisance. It was found that laser-excited Yb^{+*} in the metastable states reacts with residual H_2 molecules and forms YbH^+ [19]. This is a very serious problem for a frequency standard using buffer-gas-cooled Yb^+, since it is difficult to remove residual H_2 gas completely from vacuum systems. In the case of Ca^+, the reaction of $Ca^+ + H_2 \rightarrow CaH^+ + H$ possibly occurs

through the 4 ^2P_J states. Ca^+ ions in the metastable states, however, hardly react with H_2, since the reaction is an endothermic one of about 2 eV (see figure 2) [20]. In addition to the hydrogenation reaction, the chemical reaction with H_2O molecules is another problem for frequency standards. Since a laser-excited ion has a relatively high internal energy and an H_2O molecule has a large permanent electric dipole moment, the chemical reaction with the H_2O molecule may even be accelerated. Even when the partial pressure of H_2O is very low, the loss of trapped ions caused by this reaction is not negligible. Especially for buffer-gas-cooled ions with metastable states, the ion loss produced by this reaction may affect the lifetime and the quenching rate measurements of the metastable states. In order to determine whether the chemical reaction with H_2O has an effect on such measurements, detailed information on the process is required.

On the other hand, the hydration reaction is closely related to experiments that use a radioactive beam. We have been working on a project to study the hyperfine anomaly of unstable Be^+ and Ca^+ ions as a possible application of short-lived ions produced at a radioactive beam facility [21–23]. Generally, the unstable isotope ions are provided as energetic ion beams from an accelerator facility. Those ions, therefore, must be cooled down to thermal energy and be trapped in an ion trap in order to perform precise hyperfine spectroscopy. For this purpose, an ion guide system consisting of a helium-gas chamber is used [24, 25]. In this gas chamber, the unstable ions can collide with residual H_2O molecules that are usually present in helium gas, and form hydrated ions during cooling [26]. Thus, the hydration reaction and the dissociation of $Ca^+(H_2O)_n$ and $CaOH^+(H_2O)_n$ are important subjects for our experimental project.

In this paper, we present experimental evidence of the acceleration of the chemical reaction of trapped $^{40}Ca^+$ ions with H_2O molecules by laser excitation. The reaction-product ions were sympathetically cooled by laser-cooled $^{40}Ca^+$ ions and were sensitively detected by laser-induced fluorescence mass spectroscopy. This method allows the observation of the signal of the products even in ultrahigh vacuum. The reaction rate coefficient and its temperature dependence were also measured for buffer-gas-cooled $^{40}Ca^+$ ions.

2. Apparatus

A schematic diagram of the experimental set-up is shown in figure 1 [27]. The linear trap consists of three sections each made from four separate rods with a diameter of 8 mm. The closest diagonal distance $2r_0$ between the electrodes of the linear trap is 7.0 mm. The driving rf and the applied amplitude are typically 3.3 MHz and 250 V, respectively. The corresponding radial pseudopotential well is approximately 7 eV. Correction dc voltages were applied to the centre electrodes in order to optimize the ion cloud position that is sometimes displaced by patch potentials. The vacuum chamber was evacuated by a turbomolecular pump (300 l s^{-1}) backed up by a rotary pump. The residual pressure was around 1×10^{-7} Pa at room temperature. For buffer-gas cooling of trapped ions, we loaded helium gas from the fore vacuum side of the turbomolecular pump. A reservoir containing pure water was connected to a variable leak valve directly attached to the port of the trap chamber, which is about 30 cm away from the ion trap. To remove impurities in the water (mainly N_2), we repeated standard purification many times (freezing by liquid nitrogen, evacuating and melting). A partial pressure gauge (Anelva M-066QG), as well as a nude ionization gauge, was attached to the central port of the main chamber in order to check the H_2O pressure and the presence of other residual gases when introducing He and H_2O. The partial pressure gauge was calibrated to an accuracy of $\pm 10\%$ by the manufacturer, and it was placed about 15 cm away from the ion trap. In order to realize static pressure regime after changing H_2O pressure, we waited for at least 5 min before starting measurements.

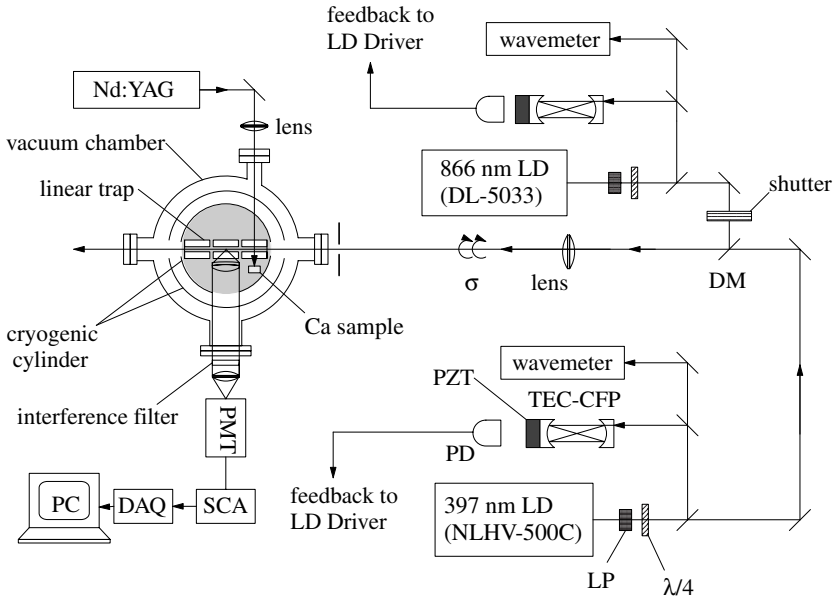

Figure 1. Experimental set-up. LD: laser diode, LP: linear polarizer, $\lambda/4$: quarter-wave plate, DM: dichroic mirror, PD: photodiode, PZT: piezoelectric actuator, TEC-CFP: temperature-stabilized confocal Fabry–Perot, DAQ: data acquisition card, SCA: single-channel analyser, PMT: photomultiplier tube.

The laser-ablation method was used for producing and trapping the Ca^+ ions. A Nd:YAG pulsed laser light (NewWave Research ACL-1) was focused onto a metallic calcium sample mounted on the side of the ion trap, and the laser-ablated Ca^+ ions were directly trapped. The storage time of the trapped Ca^+ ions extended over several hours under room-temperature conditions.

The low-lying energy level diagram of $^{40}Ca^+$ is shown in figure 2. The Ca^+ has metastable D states from which the excited P states can be accessed by the E1-allowed optical transitions. The lifetimes of the metastable D_J ($J = 3/2, 5/2$) states were measured to be about 1s [28–32]. Since the lifetime of the $P_{1/2}$ states is 7.098(20) ns [33] and the branching ratio $A(4\,^2P–4\,^2S_{1/2})/\Sigma_J A(4\,^2P–3\,^2D_J)$ of the transition probabilities is 17.6 ± 2.0 [34], the optical pumping into the D states is easily realized simply by laser excitation of the S–P transition. For laser cooling and detection of laser-induced fluorescence (LIF), we used commercial laser diodes with oscillation wavelengths of 397 and 866 nm. The violet laser excites the $4\,^2S_{1/2}$–$4\,^2P_{1/2}$ optical transition for laser cooling and the simultaneous detection of fluorescence photons. An IR laser was used to prevent optical pumping into the $3\,^2D_{3/2}$ state. Each laser diode was frequency stabilized to a temperature-controlled reference cavity. The two laser beams were merged by a dichroic mirror and directed into the ion trap through a view port window. The beam diameters at the trap centre were less than 1 mm. A mechanical shutter was inserted in the optical path of the IR laser beam for the measurement of the reaction rate. Fluorescent photons from the trapped Ca^+ ions were collected by lenses mounted near the centre of the ion trap, and focused onto a photomultiplier tube (Hamamatsu R464) by a lens placed outside the vacuum chamber. An interference filter with about 50% transmittance at 397 nm was inserted in the optical system in order to reduce stray light photons. The detection efficiency was estimated to be 1×10^{-3} by a Monte Carlo simulation of the number of photons transmitted through the optical system.

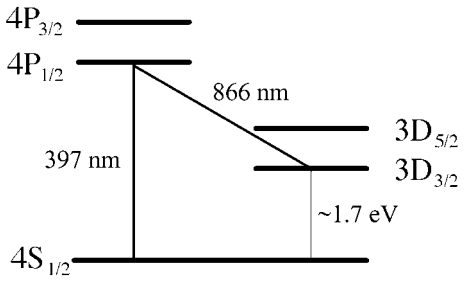

Figure 2. Simplified energy level diagram of $^{40}Ca^{+}$ (not to scale).

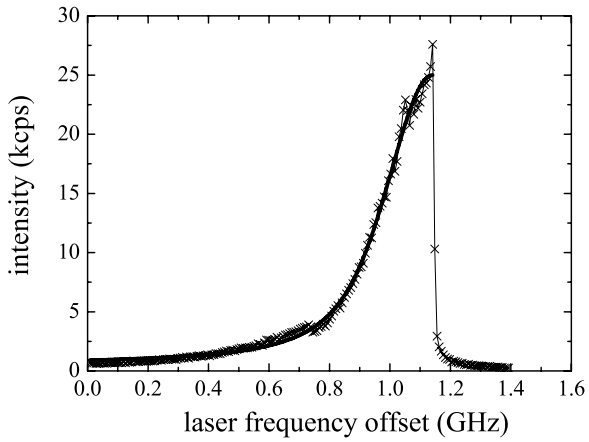

Figure 3. Laser cooling spectrum of trapped $^{40}Ca^{+}$ ions. The thick curve is obtained by fitting the Voigt profile to part of the spectrum data. The estimated half-width of the Gaussian part is 187 MHz (HWHM). The experimental parameters are: rf $f_{rf} = 3.222$ MHz, rf voltage $V_{ac} = 150$ V. The violet and IR lasers were set at $I_V = 15$ μW and $I_{IR} = 2.6$ mW, respectively.

A typical fluorescence spectrum of the laser-cooled Ca^{+} is shown in figure 3. The half width at half maximum (HWHM) of the Gaussian part is obtained to be about 187 MHz by fitting the Voigt profile to part of the spectrum data. The corresponding ion temperature in the laser beam direction is about 19 K.

3. Method of observation

LIF mass spectroscopy for trapped ions was developed, i.e., a combination of the observation of LIF and secular motion excitation by a small perturbation rf voltage [10, 11, 35]. The secular motion frequency (f_s) of a single ion is approximately given by [36]

$$f_s = \frac{\Omega}{4\pi}\sqrt{a + \frac{q^2}{2}}, \tag{1}$$

$$a = \frac{4eV_{dc}}{mr_0^2\Omega^2}, \qquad q = \frac{2eV_{ac}}{mr_0^2\Omega^2}, \tag{2}$$

where the constants m and e are the mass and charge of the trapped ion, r_0 is the geometric parameter of the linear trap, $\Omega/2\pi$ and V_{ac} are the frequency and amplitude of the driving rf amplitude for the linear trap, and V_{dc} is the dc voltage between adjacent trap electrodes.

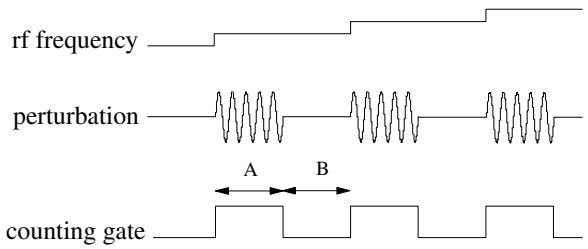

Figure 4. The time sequence of the LIF mass spectroscopy. Periods A (heating time) and B (cooling time) were set at 0.1–1.0 s to optimize the observation.

A small perturbation rf voltage $V_s \sin \omega t$ was applied to one of the trap electrodes for dipolar excitation of the secular motion. When the perturbation is in resonance with the frequency of equation (1), it selectively excites ions with a particular m/e, thus heating these ions. The ions, in turn, modify the intensity of the observed LIF from the laser-cooled Ca^+ ions through Coulomb interaction. If we scan the frequency of the perturbation, a mass spectrum can be obtained in the form of intensity changes in the fluorescence. In this experiment, the 397 nm laser frequency was detuned by a few hundred MHz on the lower side of the resonance in the $S_{1/2}$–$P_{1/2}$ transition in order to laser cool the $^{40}Ca^+$ ions, and thereafter the frequency of the perturbation rf voltage was scanned. The measurement sequence is shown in figure 4. We pulsed the perturbation rf voltage to avoid excess heating of the trapped ions and to obtain a symmetric spectrum. This method was used for the detection and mass analysis of ions produced by the chemical reaction with H_2O. For calibration of the mass spectrum, we measured the mass spectrum of $^{40}Ca^+$ ions after every run of the measurements.

4. Results

4.1. Elimination of impurity ions

We obtained a mass spectrum right after the Ca^+ ions were loaded into the trap (see figure 5(a)). In this measurement, we intentionally introduced H_2O gas at a partial pressure of 1.1×10^{-6} Pa. There were three dips in the spectrum around $M = 58$, 44 and 40. In order to avoid excess heating, the perturbation amplitude was decreased when the $^{40}Ca^+$ spectrum was measured. The signal around $M = 44$ is due to the isotope ions of $^{44}Ca^+$, which have a natural abundance of about 2%. The signal around $M = 57, 58$ is caused by sympathetic heating by the reaction-product ions between laser-ablated Ca^+ ions and H_2O molecules. These ions were produced by kinetic collisions during the trapping process.

In order to clean up the initial impurity ions, we sequentially applied a strong rf perturbation resonant with the motional frequencies of $M = 58$, 57 and 44 ions. Figures 5(b) and (c) show that this successfully removed the two signals. In the following experiments, this clean-up method was used to initialize the experiments.

4.2. Acceleration of the $Ca^+ + H_2O$ reaction

The experimental binding energy of $Ca^+(H_2O)$ is about 1.2 eV [37]. Thus, it is expected that the reaction progresses automatically for trapped Ca^+ ions by simply introducing H_2O. However, our experiments show that the reaction rate strongly depends on the state of the Ca^+ ion. The measurements were performed in the following way. The relative number of molecular ions produced within a certain reaction period under a certain partial pressure of H_2O

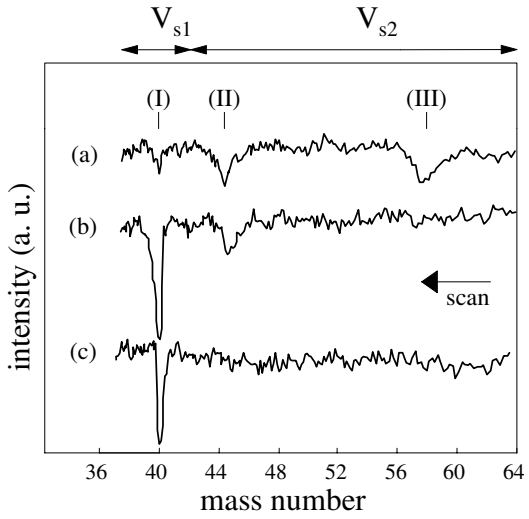

Figure 5. Demonstration of the sequential elimination of sympathetically cooled impurity ions produced during the initial stage of the trapping process. The arrow indicates the scan direction. The H_2O pressure was 1.1×10^{-6} Pa. Ca^+ ions were loaded only once. (a) Mass spectrum measured right after Ca^+ ions were loaded into the trap by the laser-ablation method. There are three dips in the spectrum around $M = 58$, 44 and 40. (b) Mass spectrum after applying a strong perturbation resonant with the motional frequencies for $M = 57$, 58 ions. The perturbation amplitude for the complete elimination of such ions was $V_s = 500$ mV. (c) Mass spectrum after eliminating the $^{44}Ca^+$ ions. The vertical scale is the same in all three spectra. Experimental parameters are as follows: driving rf $f_{rf} = 3.223$ MHz, $V_{ac} = 246$ V, $V_{dc} = 0$ V, 397 nm laser power $I_V = 20$ μW, 866 nm laser power $I_{IR} = 1.8$ mW. The perturbation amplitude V_s was set at $V_{s1} = 0.4$ mV for signal (I) and at $V_{s2} = 5.0$ mV for (II) and (III).

molecules was detected by the mass measurement method described above. After confirming the disappearance of the signal around $M = 57$ and 58, only the IR laser was turned off. A short while later, the perturbation rf was scanned to obtain a mass spectrum, a typical example of which is shown in figure 6. The H_2O pressure was set at 1.1×10^{-6} Pa. In spite of a very short reaction time of 60 s compared with the ion trapping lifetime, a strong signal was obtained. In this measurement, the perturbation frequency was scanned over a wide range for convenience of mass calibration. The amplitude V_s was reduced when measuring the $^{40}Ca^+$ spectrum. In order to experimentally check the dependence of the reactivity on the Ca^+ state during the reaction, two different ion states were prepared:

(1) ions in the $4\ ^2S_{1/2}$ states (i.e., all lasers are turned off),
(2) ions pumped into the $3\ ^2D_{3/2}$ state through the $4\ ^2P_{1/2}$ state.

As shown in figure 7, a signal was observed only when the IR laser was turned off. Although the reaction time was only 120 s, the signal in figure 7(b-2) is rather deep. On the other hand, there was no signal when both lasers were turned off for the same period (figure 7(a-2)). These measurements were performed sequentially as (a-1) $\rightarrow$ (a-2) $\rightarrow$ (b-1) $\rightarrow$ (b-2) over a period of 15 min. The spectra shown in figure 7 give clear evidence of the acceleration of the chemical reaction with H_2O by laser excitation. Note that the fluorescence intensity does not return to the original level when the ions are pumped into the D state. This fact can be used to measure the reaction rate coefficient for buffer-gas-cooled Ca^+ ions (see the next section). The above experimental results show that the chemical reaction of $Ca^{+*}(D_J)$

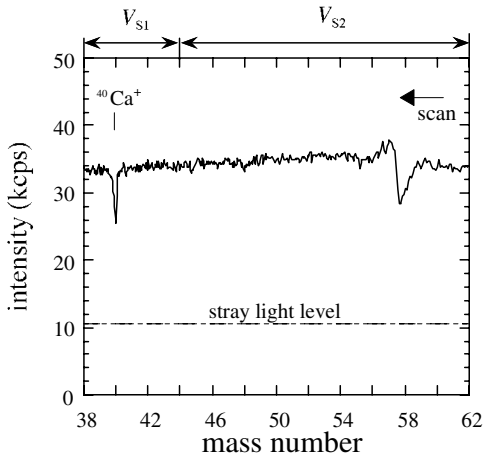

Figure 6. Signal of the reaction-product ions strengthened by introduction of H_2O. The reaction time corresponding to the IR laser-off period was set at 60 s. Experimental parameters: the perturbation amplitude was set at $V_{s2} = 5.0$ mV for $M = 57, 58$ and at $V_{s1} = 0.4$ mV for $M = 40$. $I_V = 72\ \mu$W, $I_{IR} = 1.8$ mW. The H_2O pressure was 1.1×10^{-6} Pa. The other parameters were the same as presented in figure 5.

with H_2O is clearly very fast compared with that of the ions in the ground state. The reason can be explained by the energy level structures of Ca^+ and $Ca^+(H_2O)$. Since the (2) $^2B_1$ and (2) $^2B_2$ states of $Ca^+(H_2O)$ are energetically close to those of the 3 ^2D_J states of Ca^+ and the calculated electron populations of the lower (1) $^2A_2$ and (2) $^2A_1$ states in $Ca^+(H_2O)$ are concentrated at the 3d orbit of Ca^+ [38], $Ca^{+*}(D_J)$ may easily turn into these excited states of $Ca^+(H_2O)$ by colliding with H_2O. Thus, new reaction channels are opened. We can expect the following processes:

$$Ca^{+*}(D_J) + H_2O \rightarrow Ca^+(H_2O)^* \rightarrow Ca^+(S_{1/2}) + H_2O, \quad (3a)$$

$$\rightarrow HCaOH^+ \rightarrow CaOH^+ + H, \quad (3b)$$

$$\rightarrow Ca^+(H_2O) + h\nu, \quad (3c)$$

where the evaporation process (3*a*) does not contribute to the ion loss. The rate of the radiative association process (3*c*) is considered to be very low [39], and thus there will be only a small contribution to the ion loss. The insertion reaction (3*b*) seems to be possible due to the high internal energy of $Ca^{+*}(D_J)$ [40, 41]. However, information on the potential energy surface of the Ca^+–H_2O system is necessary to estimate the contribution. At present, we suppose that the reaction-product ions consist of $CaOH^+$ and $HCaOH^+$ ions. Since the mass resolving power in the present measurements is limited, we could not distinguish $M = 57$ and 58 ions. We plan to perform photodissociation experiments as well as to prepare an external mass analyser in order to determine the branching ratio of the reaction.

It should be noted that the signal of reaction products as presented in figures 5–7 could be observed only when the laser-cooled $^{40}Ca^+$ ions were simultaneously trapped, while it was not observed at an initial stage of a laser cooling process or for buffer-gas-cooled ions. These findings indicate that the reaction-product ions were sympathetically cooled by the laser-cooled ions. In order to deduce the temperature of the reaction-product ions, a laser cooling spectrum of $^{40}Ca^+$ ions was measured when the reaction-product ions were simultaneously trapped (see figure 8(b)). The production and the elimination processes of sympathetically cooled ions are shown in figure 8(I), (II). After the chemical reaction with H_2O shown in figure 8(I), the

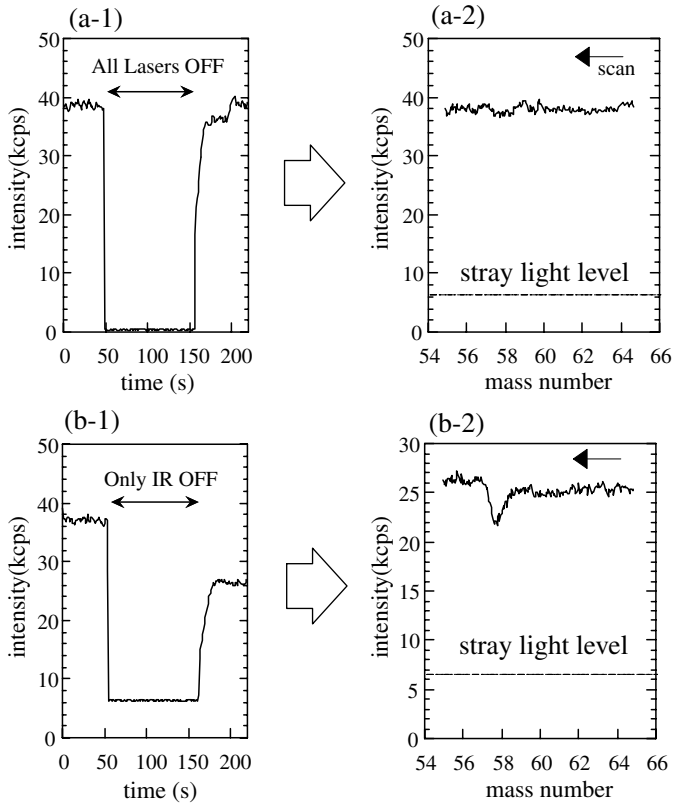

Figure 7. Dependence of the signal strength of the reaction-product ions on the Ca^+ state during the reaction time. The plots on the left and right show the time spectra of the fluorescence intensity and the observed mass spectra, respectively. (a-1) All lasers were turned off for 120 s. The fluorescence intensity returned to the original level after turning on the lasers. (a-2) Mass spectrum after procedure (a-1). There is no dip around $M = 58$. (b-1) Only the IR laser was turned off. Note that the fluorescence does not return to the original level. (b-2) Mass spectrum after procedure (b-1). These measurements were performed sequentially as (a-1) → (a-2) → (b-1) → (b-2) over a period of 15 min. The perturbation amplitude was set at $V_s = 5.0$ mV for both mass spectra. The H_2O pressure was set at 1.0×10^{-6} Pa.

ion temperature of the laser-cooled $^{40}Ca^+$ ions increased. This indicated that strong Coulomb interactions existed between the $^{40}Ca^+$ ions and the reaction-product ions. In figure 8(II), we applied the perturbation voltage at the time indicated by an arrow in order to eliminate the reaction-product ions. Since $^{40}Ca^+$ ions were efficiently laser cooled after this elimination process, an increase in the intensity was observed. Unfortunately, it is impossible to measure the fluorescence spectrum of the reaction-product ions. Thus, we estimated the ion temperature by comparing the experimental results with a molecular dynamics simulation. The simulation results show that the kinetic energies of sympathetically cooled ions are of the same order as that of the laser-cooled $^{40}Ca^+$ ions in the case of the cloud state. Although it is difficult to actually reproduce the experimental conditions, the simulation results will serve as a guide to deduce the ion temperature. Then, we assumed that the reaction-product ions were sympathetically cooled to ∼200 K in the laser beam direction.

Similar experiments were also performed under ultrahigh-vacuum (UHV) conditions of about 1×10^{-7} Pa, containing $\sim 10^{-8}$ Pa of H_2O. After the clean-up procedure, the IR laser

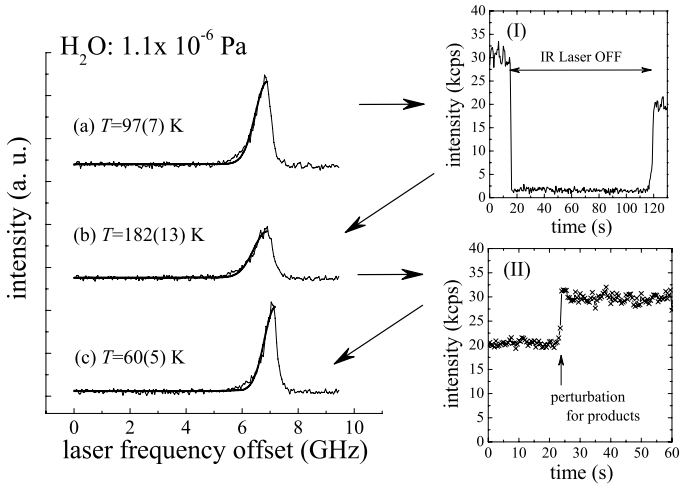

Figure 8. Fluorescence spectra from laser-cooled $^{40}Ca^+$ ions: (a) before reacting with H_2O, (b) when reaction-product ions were simultaneously trapped and (c) after the elimination of reaction-product ions. The H_2O pressure was set at 1.1×10^{-6} Pa. The vertical scale is the same in all spectra. The thick curve in each spectrum is a result of a fit of the Voigt profile to part of the spectrum from which the ion temperature of the laser beam direction is deduced. The plots on the right show the time spectra of fluorescence intensity in the production and the elimination processes of $M = 57$ and 58 ions. These measurements were performed in sequentially (a) $\rightarrow$ (I)$\rightarrow$ (b) $\rightarrow$ (II) $\rightarrow$ (c). After the reaction shown in figure (I), the fluorescence spectrum (b) was observed. The ion temperature of laser-cooled $^{40}Ca^+$ ions increased due to Coulomb interactions with reaction-product ions. The mass spectrum presented in figure 6 was also observed after reaction process (I). In figure (II), we applied a perturbation voltage ($V_s = 500$ mV amplitude) at the time indicated by an arrow in order to remove reaction-product ions of $M = 57$ and 58. An increase in the intensity was observed, since $^{40}Ca^+$ ions were efficiently laser cooled after this elimination process.

was turned off for 40 min, and then a mass spectrum was measured. A definite signal was observed around $M = 58$ (figure 9) while such a signal was not observed when both lasers were turned off for the same period. These indicate that the molecular formation reaction still has an observable probability for the ions in the D_J states even under UHV conditions.

The energy level structures of other candidates proposed as an optical frequency standard, such as Sr^+, Ba^+ and Yb^+, are similar to that of Ca^+. Moreover, their metastable energies are higher. Thus, we can expect that their chemical reaction with the H_2O molecule is also promoted by the laser excitation of their ions via a mechanism similar to that in the Ca^+ case. Sugiyama *et al* [42] reported the disappearance and shift of the rf resonance absorption signal of buffer-gas-cooled Yb^+ after introducing H_2O gas. This phenomenon could be explained by the production of $HYbOH^+$ and/or $YbOH^+$ ions. Similarly, in a single-ion experiment of Ba^+, Sankey and Madej [43] reported that an anomalous quantum jump signal was observed when introducing H_2O. This phenomenon was also explained by the chemical reaction with H_2O, as suggested in [43].

4.3. Reaction rate coefficient of $Ca^{+*}(D_J) + H_2O$

As described in the previous section, the chemical reaction of trapped Ca^+ with H_2O actively occurs when the ion is pumped into the D state. In practice, a decrease of the fluorescence intensity was observed after the IR laser was turned off, as shown in figure 7(b-1). This decrease can be attributed to ion loss by the chemical reaction with H_2O. On the other hand,

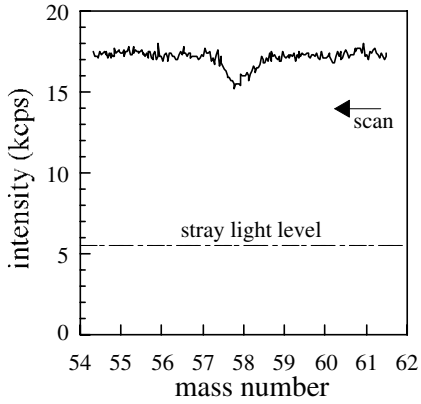

Figure 9. Observed signal of product ions due to the $Ca^{+*}(D_J)$ + H_2O reaction under UHV conditions (1×10^{-7} Pa). The partial pressure of H_2O was about 10^{-8} Pa. The reaction time corresponding to the IR laser-off period was 40 min. The experimental parameters are as follows: $I_V = 60$ μW, $I_{IR} = 2.0$ mW, perturbation amplitude $V_s = 2$ mV, $f_{rf} = 3.277$ MHz, $V_{ac} = 241$ V, $V_{dc} = -0.84$ V.

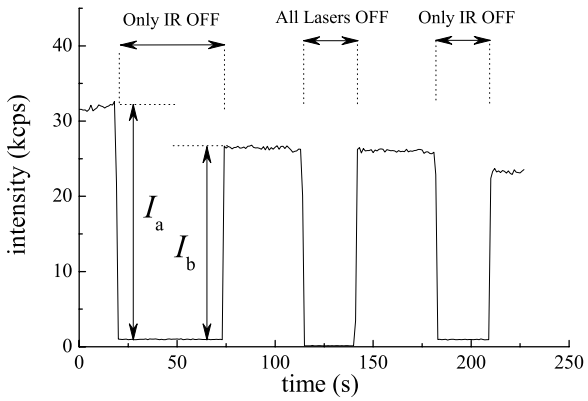

Figure 10. Decrease of fluorescence intensity from buffer-gas-cooled Ca^+ ions after the IR laser-off period. The fluorescence intensity decreases when the 866 nm laser is turned off. In these measurements, we introduced helium gas for buffer-gas cooling. The decrease in the fluorescence was caused by the chemical reaction with H_2O molecules. The experimental parameters are as follows: $I_V = 7$ μW, $I_{IR} = 1.8$ mW, He pressure 1.1×10^{-2} Pa, H_2O pressure 1.4×10^{-6} Pa, $f_{rf} = 3.223$ MHz, $V_{ac} = 246$ V, $V_{dc} = 0$.

ion losses were negligible when both lasers were turned on for fluorescence measurement. That is, we can control the chemical reaction time (t_r) of $Ca^{+*}(D_J)$ + H_2O by varying the IR laser-off period. Figure 10 shows the decrease in the fluorescence intensity after the off period of the IR laser.

Since this measurement was performed with buffer-gas-cooled ions, the fluorescence intensity is basically proportional to the number of trapped ions if the laser parameters are held constant. A small discrepancy from the linearity of the LIF intensity versus the number of $^{40}Ca^+$ ions was considered to be from the weak ion-number dependence of the line width of the fluorescence spectrum, and it was also taken into account as an additional uncertainty of the LIF as described in what follows. We define the fluorescence intensity ratio $R(t_r)$ as

$$R(t_r) = I_b/I_a. \tag{4}$$

$R(t_r)$ follows the decay curve of the trapped Ca^+ ions that decrease through the chemical reaction with H_2O. Thus, $R(t_r)$ can be expressed as

$$R(t_r) = \exp(-t_r/\tau), \tag{5}$$

$$1/\tau = k_0 n_0 + \sum_i k_i n_i, \tag{6}$$

where τ is the time constant of the decay curve, k_0 and n_0 are the reaction rate coefficient of $Ca^{+*}(D_J) + H_2O$ and the number density of H_2O, respectively, and k_i and n_i are the ith unknown reaction rate coefficient and the number density of the ith residual gas. Since the variation of the other residual gas pressures was negligible except for H_2O, $\sum k_i n_i$ was regarded as constant. Examples of decay curves of $R(t_r)$ are shown in figure 11. In these measurements, we introduced helium buffer gas as well as a relatively small amount of H_2O at the same time. We measured $1/\tau$ as a function of H_2O pressure, as shown in figure 12. From a least squares fit of equation (5) to the data in figure 12(a), we obtained the rate coefficient of $Ca^{+*}(D_J) + H_2O \rightarrow$ *products* as $k = 1.8(1) \times 10^3$ s^{-1} Pa^{-1}. The measurements were also performed for different buffer gas pressures as shown in figures 12(b) and (c) in order to clarify the residual gas effects. As assumed, the residual term $\sum k_i n_i$ was negligible and within the fitting error. In order to check the influence of the trapped ion number on the spectral width, we measured the LIF spectra at the start and the end of a series of reaction-rate measurements. Since weak dependence on the ion number was observed, a small difference of the Doppler width possibly causes an error in the LIF measurement. Accordingly, the uncertainty of the LIF intensity was evaluated from the maximum difference, and it was taken into account when calculating the intensity ratio $R(t_r)$ of equation (4). A typical error due to this effect was a few percent of the LIF intensity. On the other hand, the temperature of $^{40}Ca^+$ ions was evaluated from the experimental line widths based on the principle of equipartition of kinetic energy in all degrees of freedom. The principle may hold when trapped ions are cooled by helium buffer gas. For the case of figure 12(a), the ion temperature was evaluated to be $3.1(1) \times 10^3$ K. It is noted that this reaction rate was measured for ions pumped into both the $3\,^2D_{3/2}$ and $3\,^2D_{5/2}$ states because the fine structure mixing between these states is fast for buffer-gas-cooled ions. We estimated the population ratio $\rho(D_{5/2})/\rho(D_{3/2})$ to be about 2 by using the mixing rates given in [31, 44].

Using the same measurement procedure, the dependence of the reaction rate on the ion temperature was measured (figure 13). The ion temperature was controlled by changing the buffer gas pressure and the rf amplitude for ion trapping. The order of the reaction rate coefficient was estimated to be $\sim 10^{-11}$ cm^3 s^{-1} within this temperature range if room temperature ($T = 300$ K) was assumed for the H_2O gas. As seen in figure 13, the measured reaction rate tends to increase with decreasing ion temperature, which can be explained by the $1/\sqrt{T}$ dependence of the ion-dipole capture rate analysed in [39, 45, 46].

5. Summary

We have confirmed that the chemical reaction of trapped Ca^+ ions with the H_2O molecule is accelerated by laser excitation to the $3\,^2D_J$ ($J = 3/2, 5/2$) states. The reaction-product ions were sensitively detected by using the sympathetic cooling method. The reaction rate coefficient of $Ca^{+*}(D_J) + H_2O \rightarrow$ *products* was also measured for buffer-gas-cooled Ca^+ ions using the optical pumping technique. From the trend of the temperature dependence, we expect higher reaction rates for laser-cooled Ca^+ ions. Since the reaction-product ions never dissociate by themselves, the chemical reaction with H_2O causes an ion loss even at UHV. Thus, for single-ion spectroscopy or frequency standard applications using Ca^+, residual H_2O

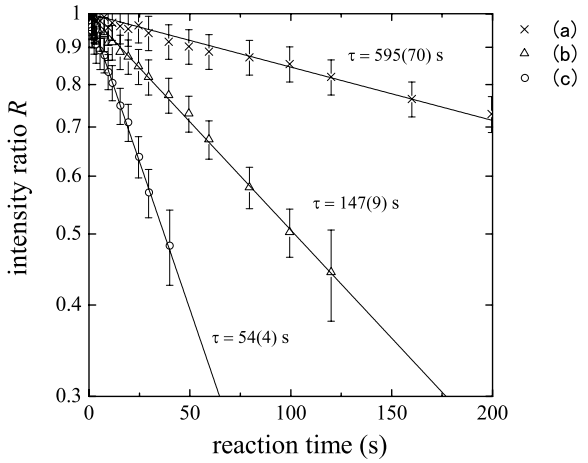

Figure 11. Decay curves of the intensity ratio as a function of reaction time. The solid lines are fits of equation (5). The time constants τ are indicated in the figure. The experimental parameters are as follows: $I_V = 15\ \mu$W, $I_{IR} = 2.0$ mW, He pressure 1.2×10^{-3} Pa, the H_2O pressure was set at (a) 1.0×10^{-6} Pa, (b) 7.0×10^{-6} Pa, (c) 1.0×10^{-5} Pa, respectively, and $f_{rf} = 3.277$ MHz, $V_{ac} = 282$ V.

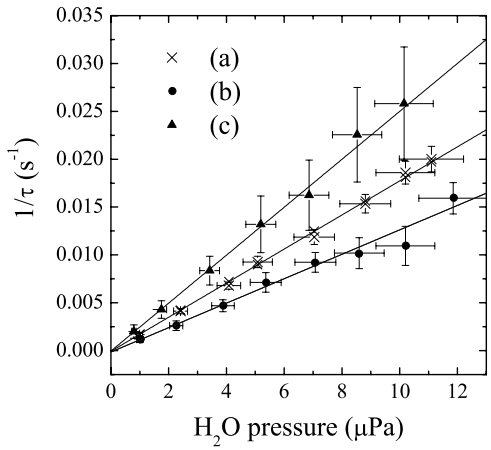

Figure 12. Plot of the decay rates of the fluorescence intensity ratio $R(t_r)$ as a function of the H_2O pressure. The experimental parameters for each data point are the same as those of figure 11 except for the helium pressure. The measurements were performed at different buffer-gas pressures of (a) 1.2×10^{-3} Pa, (b) 7.4×10^{-4} Pa and (c) 3.1×10^{-3} Pa. The measured ion temperatures were (a) $3.1(1) \times 10^3$ K, (b) $4.6(4) \times 10^3$ K and (c) $2.2(3) \times 10^3$ K.

(This figure is in colour only in the electronic version)

gas should be eliminated as much as possible. The use of a cryogenic ion trap is a possible solution [27].

Incidentally, the reaction-product ions in these experiments can become a good source of molecular ions for spectroscopic experiments by sympathetic cooling as well as photodissociation spectroscopy of single cold molecular ions, because such cold ions can easily be produced by the optical pumping technique.

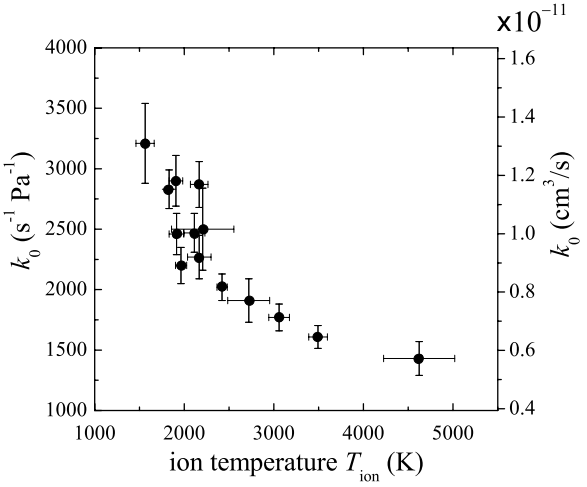

Figure 13. Dependence of the reaction rate coefficient of $Ca^{+*}(D_J) + H_2O \rightarrow$ *products* on Ca^+ ion temperature. The ion temperature was evaluated by the Doppler widths of the LIF spectra measured at the start and end of each series of measurements.

Acknowledgments

We wish to express our thanks to Professor K Fuke at Kobe University for reading the draft and making helpful suggestions. We would like to thank Dr Y Matsuo in RIKEN for helpful discussions. This work was supported by Grants-in-Aid for Encouragement of Young Scientists and for Scientific Research from the Ministry of Education, Culture, Sports, Science and Technology, and the President's Special Grant of RIKEN.

References

[1] Rafac R J, Young B C, Beall J A, Itano W M, Wineland D J and Bergquist J C 2000 *Phys. Rev. Lett.* **85** 2462
[2] Monroe C, Meekhof D M, King B E, Itano W M and Wineland D J 1995 *Phys. Rev. Lett.* **75** 4714
[3] Mitchell T B, Bollinger J J, Dubin D H E, Huang X-P, Itano W M and Baughman R H 1998 *Science* **282** 1290
[4] Block M, Drakoudis A, Leuthner H, Siebert P and Werth G 2000 *J. Phys. B: At. Mol. Opt. Phys.* **33** L375
[5] Bowe P, Hornekær L, Brodersen C, Drewsen M and Hangst J S 1999 *Phys. Rev. Lett.* **82** 2071
[6] Hornekær L, Kjærgaard N, Thommesen A M and Drewsen M 2001 *Phys. Rev. Lett.* **86** 1994
[7] Baba T and Waki I 1996 *Japan. J. Appl. Phys.* **35** L1134
[8] Van Eijkelenborg M A, Storkey M E, Segal D M and Thompson R C 1999 *Phys. Rev.* A **60** 3903
[9] Mølhave K and Drewsen M 2000 *Phys. Rev.* A **62** 011401(R)
[10] Baba T and Waki I 2002 *J. Chem. Phys.* **116** 1858
[11] Wineland D J, Bollinger J J and Itano W M 1983 *Phys. Rev. Lett.* **50** 628
[12] Larson D L, Bergquist J C, Bollinger J J, Itano W M and Wineland D J 1986 *Phys. Rev. Lett.* **57** 70
[13] Imajo H, Hayasaka K, Ohmukai R, Tanaka U, Watanabe M and Urabe S 1996 *Phys. Rev.* A **53** 122
[14] Blinov B B, Deslauriers L, Lee P, Madsen M J, Miller R and Monroe C 2002 *Phys. Rev.* A **65** 040304-1
[15] McEwan M J, Scott G B I and Anicich V G 1998 *Int. J. Mass Spectrom. Ion Process.* **172** 209
[16] Luine J A and Dunn G H 1985 *Astrophys. J.* **299** L67
[17] Church D A 1993 *Phys. Rep.* **228** 253
[18] Gerlich D 1995 *Phys. Scr.* T **59** 256
[19] Sugiyama K and Yoda J 1997 *Phys. Rev.* A **55** R10
[20] Georgiadis R and Armentrout P B 1988 *J. Phys. Chem.* **92** 7060
[21] Wada M *et al* 1997 *Nucl. Phys.* A **626** 365c
[22] Wada M *et al* 2000 *RIKEN Rev.* **31** 56

[23] Okada K, Wada M, Nakamura T, Iida R, Ohtani S, Tanaka J, Kawakami H and Katayama I 1998 *J. Phys. Soc. Japan* **67** 3073
[24] Wada M *et al* 2002 *Proc. Int. Workshop on Non-Neutral Plasmas (San Diego, CA) (Non-Neutral Plasma Physics vol 4* (AIP CP606) (New York: American Institute of Physics) p 625
[25] Wada M *et al* 2002 *Proc. 14th Int. Conf. on Electromagnetic Isotope Separators and Techniques Related to their Applications Nucl. Instrum. Methods* B at press
[26] Fujitaka S *et al* 1997 *Nucl. Instrum. Methods* B **126** 386
[27] Okada K, Wada M, Nakamura T, Katayama I, Boesten L and Ohtani S 2001 *Japan. J. Appl. Phys.* **40** 4221
[28] Ritter G and Eichmann U 1997 *J. Phys. B: At. Mol. Opt. Phys.* **30** L141
[29] Block M, Seibert P, Rehm O and Werth G 1999 *Eur. Phys. J.* D **7** 461
[30] Urabe S, Hayasaka K, Watanabe M, Imajo H, Ohmukai R and Hayashi R 1993 *Appl. Phys.* B **57** 367
[31] Knoop M, Vedel M and Vedel F 1995 *Phys. Rev.* A **52** 3763
[32] Arbes F, Gudjons T, Kurth F, Werth G, Marin F and Inguscio M 1993 *Z. Phys.* D **25** 295
[33] Jin J and Church D A 1993 *Phys. Rev. Lett.* **70** 3213
[34] Gallagher A 1967 *Phys. Rev.* **157** 24
[35] Nakamura T, Ohtani S, Wada M, Okada K, Katayama I and Schuessler H A 2001 *J. Appl. Phys.* **89** 2922
[36] Wuerker R F, Shelton H and Langmuir R 1959 *J. Appl. Phys.* **30** 342
[37] Kochanski E and Constantin E 1987 *J. Chem. Phys.* **87** 1661
[38] Bauschlicher C W Jr, Sodupe M and Partridge H 1992 *J. Chem. Phys.* **96** 4453
[39] Bates D R 1983 *Astrophys. J.* **270** 564
[40] Sanekata M, Misaizu F and Fuke K 1996 *J. Chem. Phys.* **104** 9768
[41] Hrušák J, Stöckigt D and Schwarz H 1994 *Chem. Phys. Lett.* **221** 518
[42] Sugiyama K and Yoda J 1995 *Japan. J. Appl. Phys.* **34** L584
[43] Sankey J D and Madej A A 1990 *Appl. Phys.* B **50** 433
[44] Knoop M, Vedel M and Vedel F 1998 *Phys. Rev.* A **58** 264
[45] Moran T F and Hamill W H 1963 *J. Chem. Phys.* **39** 1413
[46] Chesnavich W J, Su T and Bowers M T 1980 *J. Chem. Phys.* **72** 2641